Gas−Phase Mass Transfer in a Centrifugal Contactor

ARTICLE *in* INDUSTRIAL & ENGINEERING CHEMISTRY RESEARCH · NOVEMBER 2000

Impact Factor: 2.59 · DOI: 10.1021/ie0000818

3 AUTHORS:

Pavitra Sandilya
IIT Kharagpur
7 PUBLICATIONS **84** CITATIONS
SEE PROFILE

Davuluri P Rao
Indian Institute of Technology Kanpur
76 PUBLICATIONS **713** CITATIONS
SEE PROFILE

Ashutosh Sharma IITK
Indian Institute of Technology Kanpur
335 PUBLICATIONS **7,410** CITATIONS
SEE PROFILE

Gas-Phase Mass Transfer in a Centrifugal Contactor

Pavitra Sandilya, D. P. Rao,* and A. Sharma

Department of Chemical Engineering, Indian Institute of Technology, Kanpur 208016, India

G. Biswas

Department of Mechanical Engineering, Indian Institute of Technology, Kanpur 208016, India

The liquid-side mass transfer rate in a centrifugal gas−liquid contactor has been reported to be several times higher than that in conventional packed beds. However, no direct measurement of the gas-side mass transfer coefficient has been reported. We present experimental studies on gas-side mass transfer in a rotating packed bed with wire-gauze packing. Contrary to expectations, the gas-side mass transfer coefficient was much lower than that in conventional packed columns. An analysis of the gas flow, based on the equations of motion, revealed that the gas undergoes solid-body-like rotation in the rotor because of the drag offered by the packing. Therefore, the mass transfer coefficient should be in the same range as that in conventional packed columns. The lower value of the coefficient found experimentally is attributed to liquid maldistribution. The possibility of enhancing the mass transfer coefficient by enhancing the slip between the gas and the packing was explored by using a stack of closely spaced disks as the packing. Mass transfer studies with a pair of disks were conducted. Higher throughputs and mass transfer rates than those with the wire-gauze packing were obtained. A stack of disks as packing appears to hold promise.

Introduction

Liquid-phase mass transfer and hydrodynamic behavior in rotating packed beds (RPBs) have been studied extensively. Substantial enhancement in the liquid-side mass transfer coefficient has been reported.[1−6] Tung and Mah[7] correlated the mass transfer data of Ramshaw and Mallinson[1] by assuming film flow of liquid over the packing surface. The liquid flow has also been analyzed by assuming film flow over the packing surface.[2,3] The validity of this assumption has been examined by Bašić and Duduković[8] through conductivity measurements in a bed of glass beads. They concluded that the flow was predominantly in the form of radially oriented rivulates rather than isotropically distributed films. The first visual evidence of liquid maldistribution was presented by Burns and Ramshaw[9] in a bed of reticulated PVC packing. The nature of the liquid flow inside the RPB was found to depend on the nature of the packing.

The overall gas-phase mass transfer coefficient was reported by Liu et al.[10] based on their experiments involving the stripping of ethanol from a ethanol−water mixture using elliptic cylindrical and rectangular plastic beads. The transfer coefficient was found to increase with rotational speed. The mass transfer and hydrodynamic data for distillation in the RPB were reported for the first time by Kelleher and Fair.[11] They determined the overall mass transfer coefficient and deduced the gas-side mass transfer coefficient by deducting the liquid-side mass transfer coefficient calculated from the correlation proposed by Singh et al.[6] They found the gas-side mass transfer coefficient to increase with the rotational speed. However, there has been no direct measurement of the gas-side mass transfer coefficient.

* To whom correspondence should be addressed. E-mail: dprao@iitk.ac.in. Phone: (91)(0512)597873. Fax: (91)(0512)-590260.

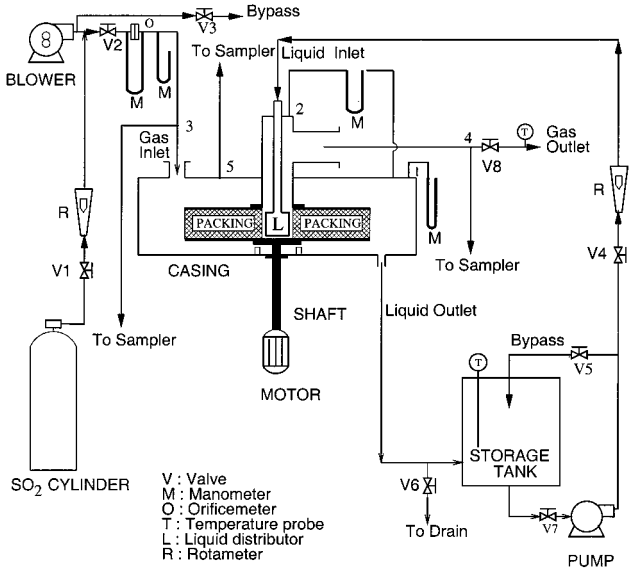

Figure 1. Schematic of the experimental setup.

This aspect needs to be studied as the gas-side resistance is important in many gas−liquid separation processes.

The twin objectives of the present study are (i) to obtain the gas-side mass transfer coefficient and (ii) to examine the effect of rotation and packing on the gas flow and the transfer coefficient.

Experimental Section

Figure 1 shows the schematic diagram of the experimental setup. The contactor consisted of a rotor housed in a casing made from transparent acrylic sheets to aid in visual observation. The rotor was driven by an AC induction motor whose speed was set using an inverter

10.1021/ie0000818 CCC: $20.00
Published on Web 00/00/0000 **PAGE EST: 8.1**

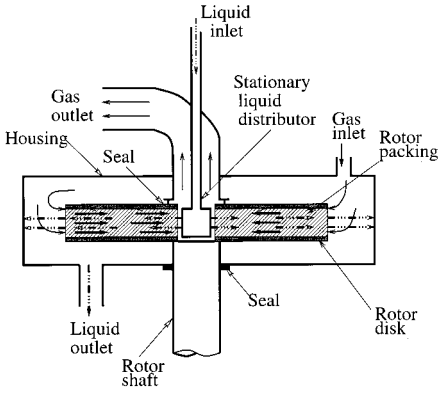

Figure 2. Schematic of the RPB unit.

drive. The other details are given in Figure 1. A schematic diagram of the contactor is shown in Figure 2. It consisted of a pair of $^1/_2$-in.-thick concentric transparent acrylic disks of 31 cm diameter. The top disk had a concentric hole of 6 cm diameter to accommodate the gas outlet pipe (5 cm diameter, made of brass). A copper tube (1.5 cm diameter) was coaxially secured inside this pipe for introduction of the liquid. The disk spacing was kept at 2.22 cm by fastening the disks coaxially using spacers. The packing, in the form of a stack of 15 circular stainless steel wire meshes, was kept between the two disks. The wire meshes had the same inner and outer radii as the rotor. The wire strands were 0.5 mm in diameter. This gave a packed bed with a porosity and specific surface area of 0.91 and 2196 m^2/m^3, respectively. The rotor was mounted on a steel shaft supported vertically with a bearing arrangement. The casing had a circular base onto which 12 rectangular plates were glued in the form of a regular polygon. Another circular plate was screwed to the top edge of these plates. The gas outlet was provided with a mechanical sealing assembly to avoid bypassing of the gas from the casing into the gas outlet. A liquid distributor (L, 2.9 cm diameter) was welded to one end of the liquid inlet tube. The distributor was a hollow cylinder and had four sets of holes separated by 90°. Each set had four equally spaced holes of 0.5 mm diameter spaced vertically on the distributor wall.

The gas was introduced into the casing through an acrylic pipe (5.8 cm diameter) fitted to the top plate. It then flowed radially inward through the rotor under an imposed pressure gradient. The liquid traveled outward through the rotor because of centrifugal force and collected on the casing bottom and flowed into the storage tank by gravity.

The gas flow rate was measured by an orifice meter made as per the ASTM specifications.[12] The liquid flow rate was monitored using a rotameter. The pressure drop across the rotor was measured with an inclined manometer. The rotor speed was measured using a stroboscopic tachometer. The same liquid flow rate (14 mL/s) was used in all of the runs, as the liquid-side resistance was negligible. To collect the gas samples, cylindrical glass samplers were used. One end of each sampler was provided with a stopcock. The sampler was initially filled with water. While the gas was being collected, the stopcock was opened to allow the gas to fill the sampler by displacement of the water. The sampler was purged with the gas for some time after the water had drained out. A known amount of sodium hydroxide solution with 0.5 vol % glycerine was then added, and the mixture was shaken vigorously to absorb SO_2 in the solution. Glycerine helped in fixing the sulfite formed by preventing the formation of sulfate on oxidation of sulfite.[13] The sulfite was analyzed by iodometry to determine the SO_2 concentration. The details can be found elsewhere.[14]

It is shown later that the gas rotates along with the rotor because of the drag offered by the packing. Therefore, to reduce the drag and to retain a large specific surface area, the use of a stack of smooth disks was conceived. Considering a pair of disks as a unit of the stack, hydrodynamic and mass transfer studies were carried out with the rotor having a pair of smooth disks.

Three different configurations with the two smooth disks were used: (i) both of the disks rotating, (ii) upper disk stationary and lower disk rotating, and (iii) upper disk stationary with turbulence promoter and lower disk rotating. In all cases, the disk spacing was kept at 2 mm to have a large interfacial area per unit volume of the rotor, and the lower disk was mounted on the rotating shaft. The two rotating disks (configuration i) were held together using four spacers placed 90° apart at the outer periphery of the rotor. In case of configurations ii and iii, the upper disk was held stationary by securing it with the gas outlet pipe after removing the spacers. These configurations were used to explore the effects of tangential shear and turbulence promoters on the mass transfer rate. Six strips of acrylic with square teeth (1 mm in each height and width and separated by 1 mm) were used as turbulence promoters. These strips were fixed in the grooves on the upper disk. A few of the holes in the distributor were blocked to keep the remaining ones inline with the flow area at the inner periphery of the rotor. The effective porosity and the specific surface area were unity and 1000 m^2/m^3, respectively.

Analysis of the Pressure Drop

The gas pressure drop across the unit, ΔP_t, was analyzed to deduce the friction factor. This was done by resolving the measured gas pressure drop into two broad components, ΔP_a and ΔP_o. The pressure drop ΔP_a consists of the centrifugal drop, frictional loss, and pressure drop due to momentum increase as the gas flows through the rotor; ΔP_o consists of the entry and exit losses at the outer and inner periphery of the rotor, respectively, and the drop due to momentum change as the gas enters the outlet pipe from the inner periphery of the rotor.

Determination of ΔP_o. In the casing, the gas is assumed to rotate with the angular velocity of the rotor (except in the vicinity of the casing wall, as the velocity is zero at the wall). The pressure drop between the gas inlet and the outer periphery of the rotor was measured and found to be negligible. On leaving the rotor, the gas flow may expand or contract depending on the relative magnitudes of the flow area at the inner periphery of the rotor and that of the outlet line. Further, the gas is expected to continue to rotate as it leaves the rotor. This could give rise to a pressure gradient. However, this component could not be estimated and, therefore, was a source of uncertainty in the determination of ΔP_o. With these considerations, ΔP_o is resolved into two main components, one due to contraction or expansion as the case may be and the other due to momentum change as the gas flows from the inner periphery of the rotor into the outlet line. Thus

$$\Delta P_o = \frac{1}{2}\rho_g K V_i^2 + \frac{1}{2}\rho_g (V_e^2 - V_i^2) \quad (1)$$

where ρ_g is the density of the gas, K is the contraction or expansion coefficient at the inner periphery of the rotor, V_e is the gas velocity in the outlet line (the annular space between the outlet pipe and the liquid inlet tube), V_i is the superficial gas velocity at the inner periphery of the rotor. The coefficient K was taken as 0.5 for both contraction and expansion. Alhough the value selected for K is questionable, it is shown later that it had no effect on the conclusions drawn, as these losses were negligible.

Determination of ΔP_a. The pressure drop across the rotor can be determined from the radial component of the equations of motion expressed in terms of the axial-average velocities. Assuming steady, incompressible, axisymmetric flow and zero axial velocity of the gas, the radial equation of motion in cylindrical coordinates can be reduced to

$$-\frac{dP}{dr} = \rho_g \left[\underbrace{-\frac{\bar{V}_r^2}{r}}_{1} \underbrace{-\frac{\bar{V}_\theta^2}{r}}_{2} \underbrace{-\frac{1}{2} f_r \frac{\bar{V}_r^2}{d_h}}_{3} \right] \quad (2)$$

where d_h is the hydraulic diameter; $\bar{V}_r$ and $\bar{V}_\theta$ are axial-average interstitial radial and tangential velocities, respectively, of the gas; and f_r is the friction factor in the radial direction. In eq 2, term 1 denotes the pressure drop due to momentum gain as the gas accelerates from the outer to the inner periphery of the rotor, term 2 represents the centrifugal pressure drop, and term 3 accounts for the frictional pressure drop. It is seen that ΔP_a can be calculated once $\bar{V}_r$ and $\bar{V}_\theta$ are known. The interstitial velocity $\bar{V}_r$ can be found from the continuity equation as

$$\bar{V}_r = \frac{Q_g}{2\pi r a \epsilon} \quad (3)$$

where Q_g is the volumetric gas flow rate; a is the axial height between the disks; and ϵ is the porosity of the RPB, which is unity for the two rotating disks. The tangential equation of motion can be reduced to

$$\frac{d\bar{V}_\theta}{dr} = \frac{1}{2} f_\theta \frac{\bar{V}_\theta - \omega r}{d_h \bar{V}_r} |\bar{V}_\theta - \omega r| - \frac{\bar{V}_\theta}{r} \quad (4)$$

where f_θ is the friction factor in the tangential directions. Equations 2 and 4 can be solved for P and $\bar{V}_\theta$ using the following initial conditions

$$\text{at } r = r_o, \quad P = P_o, \bar{V}_\theta = \omega r_o \quad (5)$$

where P_o is the pressure at the outer periphery of the rotor.

The pressure drop due to momentum gain, ΔP_m, can be obtained by integrating term 2 in eq 2 as

$$\Delta P_m = \rho_g \int_{r_i}^{r_o} \frac{\bar{V}_r^2}{r} dr \quad (6)$$

Substituting eq 3 in eq 6 and integrating, we get

$$\Delta P_m = \frac{1}{2}\rho_g \left(\frac{Q_g}{2\pi a \epsilon} \right)^2 \left(\frac{1}{r_i^2} - \frac{1}{r_o^2} \right) \quad (7)$$

The centrifugal pressure drop, ΔP_c, can now be evaluated from

$$\Delta P_c = \rho_g \int_{r_i}^{r_o} \frac{\bar{V}_\theta^2}{r} dr \quad (8)$$

To obtain the frictional pressure drop, ΔP_f, the gas was considered to take a spiral path through the rotor. Hence, the friction factor is defined in terms of the relative velocity of the gas with respect to the rotor, V_{rel}. Also the actual path, S, traversed by the gas should be more than the radial span ($r_o - r_i$). Thus

$$dP_f = \frac{1}{2} f_r \rho_g \frac{V_{rel}^2}{d_h} dS \quad (9)$$

where

$$V_{rel} = \sqrt{\bar{V}_r^2 + (\bar{V}_\theta - \omega r)^2} \quad (10)$$

However, as will be shown later, $\bar{V}_\theta$ was marginally different from ωr. Hence, for the sake of simplification, we have set $V_{rel} \approx \bar{V}_r$ and reduced eq 9 to

$$dP_f = \frac{1}{2} f_r \rho_g \frac{\bar{V}_r^2}{d_h} dr \quad (11)$$

Because the gas velocity increases in the flow direction, the friction factor is also expected to vary radially. Kelleher and Fair[11] used the functional form of the Ergun equation to account for the local variation of friction factor. We adopted the following forms for f_r

$$f_r = \begin{cases} \dfrac{\alpha}{\mathrm{Re}} + \beta & \text{for RPB} \\ \dfrac{\alpha}{\mathrm{Re}} & \text{for two rotating disks} \end{cases} \quad (12)$$

in which Re is the Reynolds number ($\langle V_r \rangle d_h / \nu_g$) and $\langle V_r \rangle$-($\epsilon \bar{V}_r$) is the superficial velocity of the gas. Substituting eq 12 into eq 11 and integrating over the radial span, we get

$$\Delta P_f = \frac{\rho_g}{2\epsilon^2 d_h} \left(\frac{Q_g}{2\pi a} \right)^2 \left[\alpha \frac{2\pi a \nu_g}{Q_g d_h} \ln \frac{r_o}{r_i} + \Phi \beta \left(\frac{1}{r_i} - \frac{1}{r_o} \right) \right] \quad (13)$$

where Φ is unity for the RPB and zero for the rotating disks. The evaluation of the friction factors is described below.

Determination of the Friction Factors. The pressure drop ΔP_o and that due to momentum gain, ΔP_m, are found from eqs 1 and 7 respectively. On subtracting these from the measured pressure drop, ΔP_t, we obtain the net pressure drop due to frictional loss and centrifugal drop ($\Delta P_f + \Delta P_c$). The evaluation of ΔP_c requires the tangential velocity of the gas, $\bar{V}_\theta$, and the friction factor, f_θ. We have assumed that the friction factors are directionally insensitive for the wire meshes and the disks, so we set $f_r = f_\theta = f$. The values of $\bar{V}_\theta$ and f are found by iteration as follows. The iteration was started by setting $\bar{V}_\theta$ to ωr. The value of ΔP_c was then calculated from eq 8, and it was deducted from the summation ΔP_c

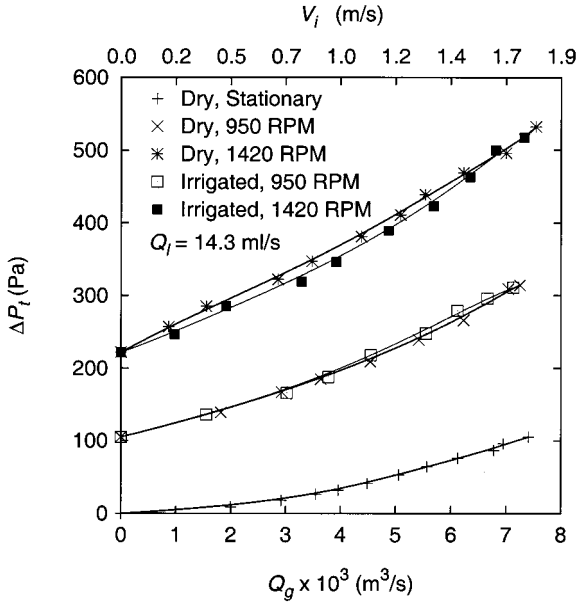

Figure 3. Variation of the total pressure drop with gas flow rate in dry and irrigated RPB.

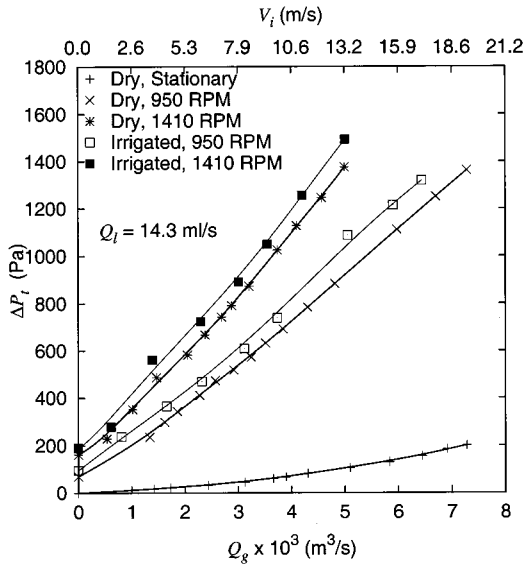

Figure 4. Variation of the total pressure drop with gas flow rate for two rotating disks.

$+ \Delta P_f$ to obtain ΔP_f. The friction factor was next found from eq 12 using the values of α and β obtained by regression analysis of eq 13. Then, V_θ (and P) was reevaluated by simultaneously solving the equations of motion, eqs 2 and 4, numerically. The iterations were continued until α and β converged.

Results and Discussion

Pressure Drop. The effects of the gas and liquid flow rates and the rotational speed on the pressure drop were studied. No flooding was observed in the experimental runs for the ranges of the parameters employed. A small amount of liquid entrainment was, however, noticed in some of the runs. The results for the RPB and the two rotating disks are presented below.

The pressure drop increased with the gas flow rate for both the RPB and the rotating disks, as shown in Figures 3 and 4, respectively. The pressure drop in the rotating rotor was more than that in the stationary one by an amount dictated by the centrifugal force. The

Table 1. Pressure Drop Components for RPB at 950 rpm in Dry Bed

	pressure drop, Pa				
	ΔP_o				
Q_g × 10^3 m^3/s	ΔP_{cont}	ΔP_l	ΔP_c	ΔP_m	ΔP_f
rotating packed bed					
0.00	0.00	0.00	127	0.00	0
1.82	0.10	0.47	129	0.00	31
3.64	0.41	1.91	131	0.01	74
5.42	0.91	4.23	133	0.02	123
7.04	1.53	7.13	134	0.03	188
two rotating disks					
0.00	0	0	131	0	0
2.92	17	−33[a]	152	33	408
4.31	37	−71[a]	163	71	642
5.98	71	−136[a]	175	137	919
7.28	105	−02[a]	185	203	1122

[a] The negative sign of ΔP_l signifies that the pressure was recovered as the flow expanded from the inner periphery of the rotor to the outlet line.

various components of the total pressure drop for the RPB and the two rotating disks are given in Table 1. For the RPB, ΔP_o and ΔP_m are negligible in comparison to ΔP_f and ΔP_c. On the other hand, all of the components are significant in the case of rotating disks.

It is also seen from Figures 3 and 4 that there is not an appreciable variation in the pressure drops of the dry bed and the irrigated bed. Keyvani and Gardner[4] reported a substantial decrease in the pressure drop by a factor of about 2 on introduction of the liquid into the bed. Recently, Zheng et al.[15] reported a similar observation. Insignificant difference in the pressure drop between the dry and irrigated beds indicates that the liquid holdup in the bed was small. The pressure drop in the case of rotating disks was found to be slightly higher with liquid flow than that in the dry rotor. This could be due to a reduction in the flow area and higher drag caused by the liquid flowing in the opposite direction. Considering the flow over flat disks, the average film thickness estimated by the method given by Munjal et al.[2] was about 0.09 mm, which is about an order of magnitude less than the disk spacing (considering that the liquid film formed on both of the confining surfaces). The flow rate is, therefore, expected to have a minor effect on the pressure drop. The difference in ΔP_t between the rotating and the stationary rotor is due to the centrifugal pressure drop. The value of ΔP_c appears to increase with the gas flow rate.

The pressure drop across the rotor would be same as the theoretical ΔP_c [i.e., $^1/_2\rho_g\omega^2(r_o^2 - r_i^2)$] if there were no gas or liquid flow (see eq 2). However, we found the experimental pressure drop to be somewhat (about 20%) lower than the theoretical ΔP_c. Although many studies[4−6,16,17] have been reported on the gas pressure drop, only Keyvani[16] reported ΔP_t with no gas and liquid flow. The experimental ΔP_t without gas and liquid flow for Keyvani[16] was more than (about twice) the theoretical ΔP_c. In the absence of the experimental data, the ratio of the experimental to the theoretical pressure drop was deduced from the correlations proposed by Kumar and Rao,[5] Singh et al.,[6] and Kelleher and Fair.[11] These values are listed in Table 2. Interestingly enough, the ratio differs from unity. The contactor can be thought to act like a blower if the ratio is more than unity and like a compressor if the ratio is less than unity. There is a need to understand the way in which the tangential velocity of the gas decays after the gas

Table 2. Comparison of Theoretical and Measured Centrifugal Pressure Drops

	ΔP_c (Pa)			
ω (rpm)	theoretical	experimental	$\Delta P_{c,exp}/\Delta P_{c,theo}$	reference
950	127	105	0.83	present work, wire mesh
1420	288	222	0.77	
950	127	70	0.55	present work, rotating disks
1420	288	162	0.56	
944	208	429	2.06	Keyvani, 1989
1253	366	731	2.00	
610	–	–	0.73[a]	Kumar and Rao, 1990
1140	–	–	0.51[a]	
100–1000	–	–	1.80[a]	Singh et al., 1992
500–1000	–	–	1.00[a]	Kelleher and Fair, 1996

[a] Deduced from the proposed pressure drop correlation.

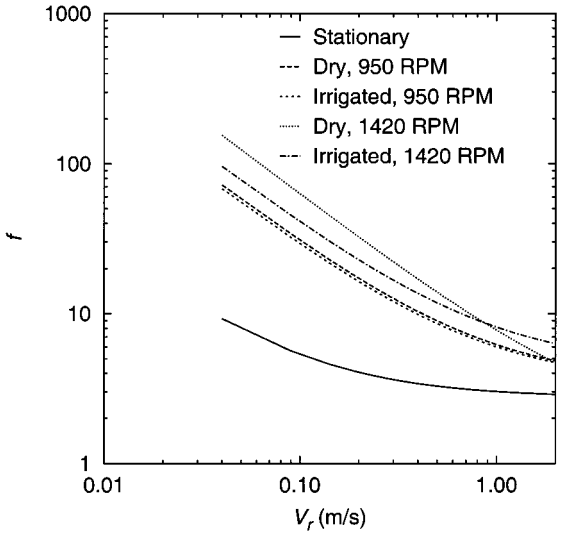

Figure 5. Variation of the local frictional factor with superficial gas velocity in the RPB.

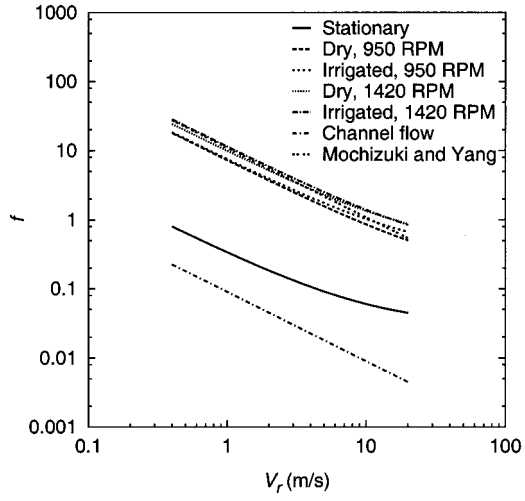

Figure 6. Variation of the local friction factor with the superficial gas velocity in two rotating disks.

leaves the rotor. This aspect requires a detailed study, as this affects the evaluation of f as well as the power requirement.

The friction factors in the case of the RPB and the rotating disks are plotted in Figures 5 and 6, respectively. It is seen that f does not vary significantly with the rotational speed. To examine this behavior in detail, the tangential slip velocity of the gas, $\bar{V}_{\theta s}$ ($\bar{V}_\theta - \omega r$) was evaluated and compared with the superficial radial velocity, $\langle V_r \rangle$, in Figure 7 for the RPB. Because of the Coriolis effect, the gas tends to rotate faster than the

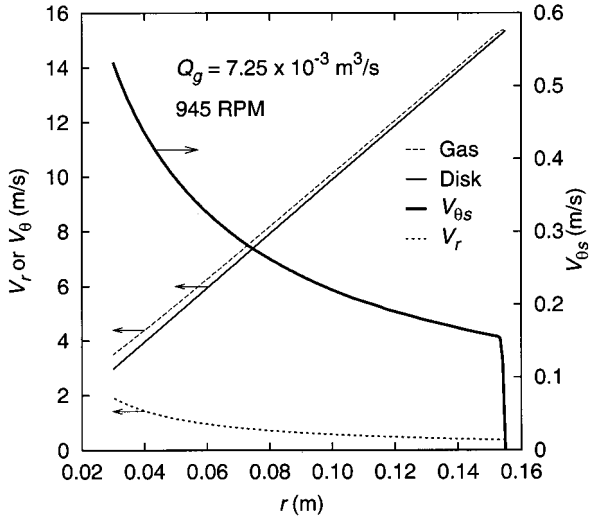

Figure 7. Comparison of $\bar{V}_r$, $\bar{V}_\theta$, and $\bar{V}_{\theta s}$ for the RPB.

disk. This behavior has also been shown by Zheng et al.[15] (see Figure 5 of their paper). The drag offered by the packing, however, retards the gas and restricts the overshoot of the gas velocity, $\bar{V}_\theta$, over the rotor speed. The $\bar{V}_r$ is much higher than $\bar{V}_{\theta s}$, and the gas can be considered to flow predominantly in the radial direction with respect to the packing. Thus, for an observer stationed on the rotor, the gas flow appears to be akin to flow in a conventional packed bed. If this were the case, then the friction factors in the rotating and the stationary rotor should be the same. We have determined the friction factor for the stationary rotor, and it is presented in Figure 5. This friction factor was substantially lower than that for the rotating case. The indirect method of evaluation of ΔP_f could have led to this lower value.

A similar trend of variation and relative magnitudes of $\bar{V}_{\theta s}$, $\langle V_r \rangle$, and f was also found for the rotating disks. Mochizuki and Yang[18] studied heat transfer enhancement in a stack of rotating annular disks and obtained the following correlation for the average friction factor for stationary disks

$$\bar{f} = \frac{1.40}{(\mathrm{Re}')^{0.222}} \tag{14}$$

where Re′ is the Reynolds number defined as $[Q_g \ln(r_o/r_i) d_h]/[2\pi a(r_o - r_i)\nu_g]$. The friction factor found with eq 14 is shown in Figure 6. Their correlation is in good agreement with the data for the rotating disks. These different trends of variation in f were attributed to the uncertainties in evaluating ΔP_f, as noted earlier. A

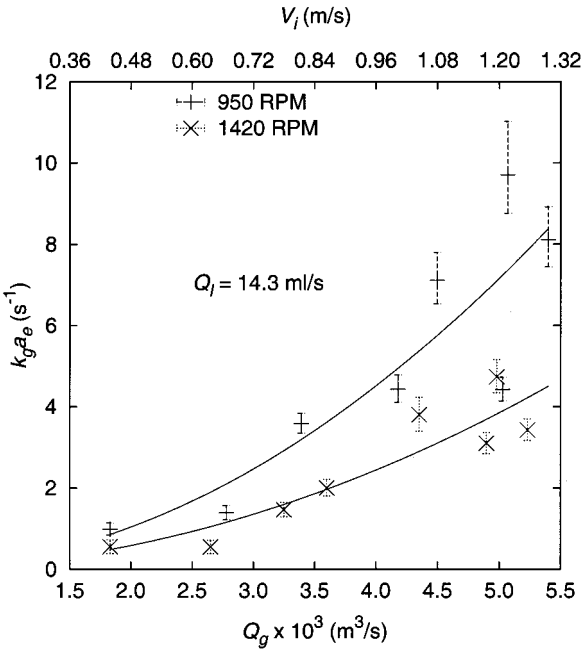

Figure 8. Variation of $\overline{k_g a_e}$ with gas flow rate for the RPB.

direct measurement of ΔP_f is, therefore, warranted to ascertain the magnitude of $\bar{V}_{\theta s}$ and to determine the variation of f with the gas velocity.

Mass Transfer. The average volumetric mass transfer coefficient, $\overline{k_g a_e}$, for the RPB was determined with the equation

$$\overline{k_g a_e} = \frac{Q_g}{\pi a} \frac{\ln(c_c/c_o)}{(r_o^2 - r_i^2)} \tag{15}$$

where c_c and c_o are the SO_2 concentrations in the casing and at the outlet, respectively. In deriving eq 15, the interfacial concentration of SO_2 is taken to be zero as SO_2 reacts with NaOH instantaneously and irreversibly. The circulation of the gas induced by the rotor was considered to maintain a uniform concentration of SO_2 inside the casing.

In the case of two rotating disks, assuming both of the confining surfaces to be uniformly wetted by the liquid, the average gas-side mass transfer coefficient, $\overline{k_g}$, is obtained from the equation

$$\overline{k_g} = \frac{Q_g \ln(c_c/c_o)}{2\pi(r_o^2 - r_i^2)} \tag{16}$$

RPB. The variation of $\overline{k_g a_e}$ with the gas flow rate at two rotational speeds in the case of the RPB is presented in Figure 8. The experimental error bounds on $\overline{k_g a_e}$, calculated based on the uncertainties in the SO_2 analysis and gas flow rate measurements, are also shown in the figure. The transfer coefficient increased with the gas flow rate. However, within the experimental accuracy, no appreciable variation in $\overline{k_g a_e}$ was observed with increasing rotational speed. This is to be expected as $\bar{V}_{\theta s}$ was negligible in comparison to $\langle V_r \rangle$.

A knowledge of the mass transfer coefficient and the interfacial area individually as opposed to $\overline{k_g a_e}$ provides better insight into the mass transfer performance of a device. Because the interfacial area was not determined in the present study, the gas-side mass transfer coefficient, $\overline{k_g}$, was estimated by considering two situations of the liquid flow. In one, the liquid is assumed to spread uniformly over the surface of a wire screen so that the liquid flow is similar to that over a plane disk. In the other, the liquid is considered to flow over the wire strands. These two cases are analogous to film flow and pore flow as reported by Burns and Ramshaw.[9] The specific surface areas in these two cases were found to be 1204 and 2196 m^2/m^3, respectively. Table 3 presents specific surface areas of the packing used and the volumetric mass transfer coefficients obtained in this work and those obtained by Kelleher and Fair[11] for the RPB, along with those of typical conventional packed beds. The data obtained in the present work are in the same range as those of Kelleher and Fair (1996). However, the transfer coefficients of the conventional packed beds are 2−4 times higher than those of the RPB. The $\overline{k_g}$ values in the RPB are much lower than those in the conventional packed beds. One would expect the $\overline{k_g}$ values for the RPB to be in the same range as those in the conventional beds because $\bar{V}_{\theta s}$ is negligible. The much lower $\overline{k_g}$ values indicate a severe maldistribution of the liquid. Recent studies by Bašić and Dudukovič[8] and Burns and Ramshaw[9] also indicate liquid maldistribution in the RPB.

Unfortunately, no data on gas-side mass transfer coefficients have been reported for packed beds with wire-mesh packing. On the other hand, such correlations have been reported for reacting systems using wire-gauze packing.[19] Such gauzes are used in the oxidation of ammonia and hydrocarbons. The following correlation for the mass transfer coefficient has been proposed for between one and seven screens, assuming plug flow of the gas through the screens

$$\gamma J_D = \frac{0.664}{(\mathrm{Re}^*/\gamma)^{0.57}} \quad (\text{for } 3 < \mathrm{Re}^* < 107) \tag{17}$$

where $J_D = \mathrm{Sh}/\mathrm{Sc}^{1/3}\mathrm{Re}^{*1/2}$, $\mathrm{Sh} = k_g d/D_g$, $\mathrm{Re}^* = d\langle V_r \rangle/\nu_g \epsilon$, $\gamma = (1 - Nd)^2$, d is the wire diameter, and N is the number of wires per unit length. Equation 17 was integrated over the radial span to calculate $\overline{k_g}$ from which $\overline{k_g a_e}$ was determined using $a_e = 2196$ m^2/m^3. The volumetric mass transfer coefficients for the gauzes were found to be far higher than those obtained for the RPB, as shown in Figure 9. This could be due to deviation of the gas flow from plug flow and severe liquid maldistribution. The gas flow through a few layers of wire screens is likely to be different from that through a bed of screens; nonetheless, high value of $\overline{k_g}$ for the gauze packing suggests the potential for achieving higher mass transfer coefficients in an RPB through the proper design of the packing.

Two Rotating Disks. The variation of $\overline{k_g}$ with the gas flow rate at the two rotor speeds for the two rotating disks is shown in Figure 10. In this case, a much wider range of gas velocities could be achieved. The transfer coefficient increased with the gas flow rate but remained almost unaffected by increases in the rotational speed. In this case too, the slip velocity in the tangential direction was substantially lower than the radial velocity. Therefore, the speed of rotation is expected to have an insignificant effect on the mass transfer coefficient.

In addition to the two rotating disks, two alternate arrangements of the rotor were employed for the mass transfer studies. In one, the rotor consisted of a station-

Table 3. Mass Transfer Performance in RPB and Conventional Columns

	packing	a_p (m^2/m^3)	system	$\overline{k_g a_e}$ s^{-1}	$\overline{k_g}^a$ $\times 10^3$ m/s	reference
packed column	#2 Intalox saddle	108	$SO_2-Na_2CO_3$	0.968	8.9	Strigle[19]
	2-in. Pall ring	102	SO_2−water	1.22−1.68	11.96−16.47	Meier et al.[20]
	Mellapak	247	SO_2−water	2.10−3.50	8.5−14.17	Meier et al.[20]
RPB	Sumitomo packing	2500	cyclohexane−*n*-heptane	1.3−7.7	0.52−3.08	Kelleher and Fair (1996)
	wire mesh	2196	SO_2−NaOH	0.56−8.20	0.25−3.73	present work

[a] Based on a_p.

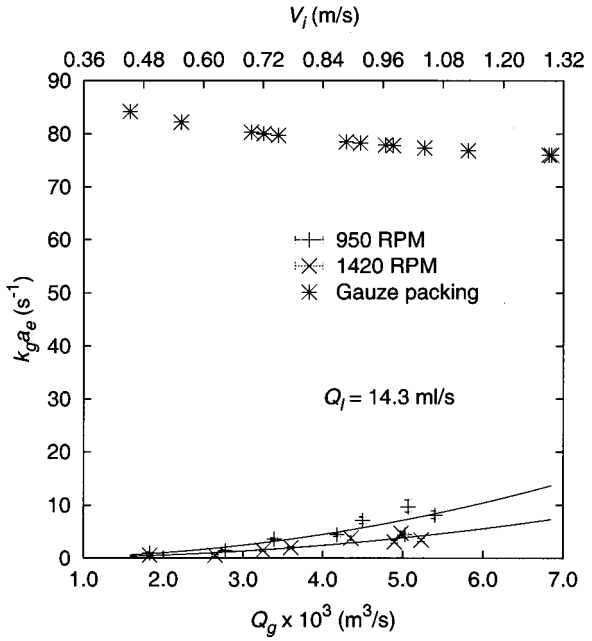

Figure 9. Comparison of $\overline{k_g a_e}$ for the RPB with that in gauze packing.

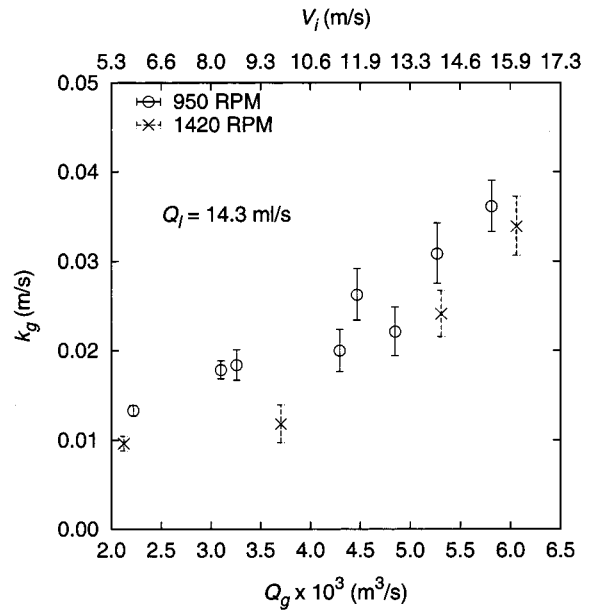

Figure 10. Variation of $\overline{k_g}$ with flow rate for two rotating disks.

ary disk and a rotating disk; in the second, the stationary disk was provided with a turbulence promoter. In these two cases, the gas is expected to experience higher shear because of the relative motion between the disks. The turbulence promoters, in the form of square teeth (1 mm long, 1 mm high, and separated by 1 mm) on

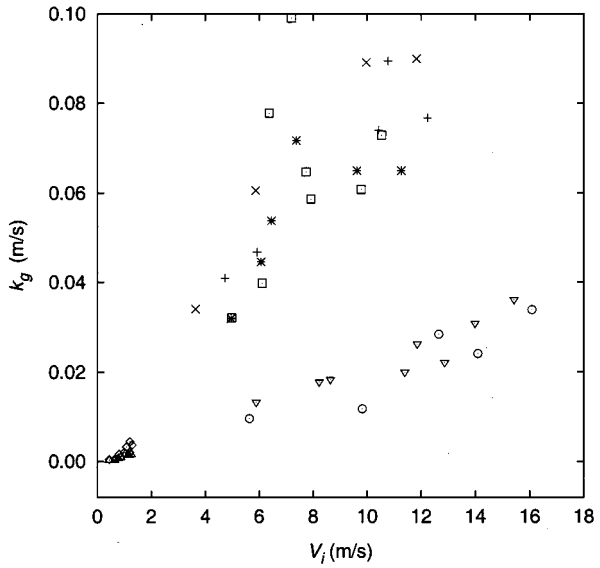

Figure 11. Comparison of $\overline{k_g}$ for various cases. +, ×: Upper disk stationary, lower disk rotating at 950 and 1420 rpm, respectively. ∗, □: Upper disk stationary with turbulence promoter, lower disk rotating at 950 and 1420 rpm, respectively. ▽, ○: Both disks rotating at 950 and 1420 rpm, respectively. ◇, ○: Rotor with wire-mesh packing rotating at 950 and 1420 rpm, respectively.

Table 4. Mass Transfer Coefficients with Different Rotors

rotor	a_p m^2/m^3	$\overline{k_g}$ $\times 10^3$ m/s	$\overline{k_g a_e}$ s^{-1}
two disks rotating	1000	0.5−35	0.5−35
one disk rotating, one disk stationary	500	10−90	5−45
one disk rotating, one disk stationary with turbulence promoter	500	30−75	15−38

thin strips of acrylic sheet, were expected to result in intermittent mixing of the gas and thus to enhance the rate of mass transfer. The turbulence promoters were placed only on the stationary disk.

The mass transfer coefficients in all of the rotor arrangements studied are presented along with the other data in Figure 11. (See also Table 4.) The gas-side mass transfer coefficient is about 2−4 times more when one disk is rotated than when both disks are rotated. The value of $\overline{k_g}$ is much higher than that in the conventional packed beds. A rotor with a stack of disks permits higher gas and liquid flow rates than an RPB without entrainment. The disk spacing can be adjusted to suit the throughputs and to achieve higher interfacial area, a flexibility that cannot be achieved with the rigid packing. Work is in progress to evaluate the efficacy of a rotor using a stack of flexible disks as packing.

Conclusions

Analysis of the pressure drop indicated that the gas undergoes a solid-body-like rotation in the RPB and, therefore, that the gas flow is akin to that in conventional packed beds. A method of evaluating the friction factor in the RPB was presented.

The gas-side volumetric mass transfer coefficient obtained in the present work is in the range of that of Kelleher and Fair.[11] In view of the negligible tangential slip velocity, the transfer coefficient should be in the range of that of the conventional packed beds, but it was found to be much lower. This result was attributed to severe liquid maldistribution in the bed. The comparison of the transfer coefficients obtained in the reacting system with those of the present work indicated a vast scope for improving the transfer rate in the RPB.

It was found that a pair of disks as a rotor permits very high throughputs of gas and liquid. The transfer coefficients were higher than those in the packed beds. It appears feasible to use a stack of closely spaced disks as a rotor and achieve high transfer rates in the centrifugal contactor.

Acknowledgment

Financial support by the Department of Science and Technology, Government of India, is gratefully acknowledged.

Nomenclature

a = axial distance between the disks of the rotor, m
a_e = effective specific surface area of the packing, m^2/m^3
a_p = specific surface area of the packing, m^2/m^3
c_c = concentration of the solute in the casing, mol/m^3
c_o = concentration of the solute at the outlet of the rotor, mol/m^3
d = diameter of wire in the gauze packing, m
D_g = diffusivity of solute gas in carrier gas, m^2/s
d_h = hydraulic diameter, $4\epsilon/a_p$, m
f = local friction factor at any radius
f_r = local friction factor in the radial direction at any radius
f_θ = local friction factor in the tangential direction at any radius
K = coefficient of contraction or expansion
J_D = J_D factor, $Sh/Sc^{1/3}Re^{*1/2}$
k_g = gas-side mass transfer coefficient at any radius, m/s
$\overline{k_g}$ = average gas-side mass transfer coefficient, m/s
$\overline{k_g a_e}$ = average gas-side volumetric mass transfer coefficient, s^{-1}
N = number of wires per millimeter of the screen, mm^{-1}
P = pressure, Pa
P_o = pressure at the outer periphery of the rotor, Pa
ΔP_c = centrifugal pressure drop, Pa
ΔP_f = frictional pressure drop, Pa
ΔP_m = pressure drop due to momentum gain, Pa
ΔP_o = pressure drop outside the rotor, Pa
ΔP_t = total pressure drop, Pa
Q_g = volumetric flow rate of gas, m^3/s
Q_l = volumetric flow rate of liquid, mL/s
r = radial coordinate
r_i = inner radius of the rotor, m
r_l = radius of the liquid tube, m
r_o = outer radius of the rotor, m
Re = Reynolds number, $\langle V_r\rangle d_h/\nu_g$
Re* = Reynolds number, $d\langle V_r\rangle/\nu_g\epsilon$
S = actual path traversed by the gas
Sc = Schmidt number, ν_g/D_g
Sh = Sherwood number, $k_g d/D_g$
V_e = gas velocity in the outlet pipe line, $Q_g/\pi(r_i^2 - r_l^2)$, m/s
V_i = superficial gas velocity at the inner periphery of the rotor, $Q_g/2\pi r_i a$, m/s
$\bar{V}_r$ = axial-averaged interstitial velocity of gas, m/s
$\langle V_r\rangle$ = superficial velocity of gas, m/s
V_{rel} = relative velocity of gas wrt the rotor, m/s
$\bar{V}_\theta$ = axial-average tangential velocity of gas, m/s
$\bar{V}_{\theta s}$ = axial-average tangential slip velocity of gas $\bar{V}_\theta - \omega r$, m/s
z = axial coordinate

Greek Symbols

$\gamma = (1 - Nd)^2$
ϵ = porosity of packing
ν_g = kinematic viscosity of gas, m^2/s
ω = rotational speed, rad/s
ρ_g = density of gas, kg/m^3

Subscripts

g = gas
i = inner periphery of rotor
l = liquid
o = outer periphery of the rotor
r = radial direction
θ = tangential direction
z = axial direction

Literature Cited

(1) Ramshaw, C.; Mallinson, R. H. Mass Transfer Process. U.S. Patent 4,283,255, 1981 (as cited by Tung and Mah, 1985).

(2) Munjal, S.; Duduković, M. P.; Ramachandran, P. Mass Transfer in Rotating Packed Beds—I. Development of Gas−Liquid and Liquid−Solid Mass-Transfer Correlations. *Chem. Eng. Sci.* **1989**, *44*, 2245.

(3) Munjal, S.; Duduković, M. P.; Ramachandran, P. Mass Transfer in Rotating Packed Beds — II. Experimental Results and Comparison with Theory and Gravity Flow. *Chem. Eng. Sci.* **1989**, *44*, 2257.

(4) Keyvani, M.; Gardner, N. C. Operating Characteristics of Rotating Beds. *Chem. Eng. Prog.* **1989**, *85*, 48.

(5) Kumar, M. P.; Rao, D. P. Studies on High-Gravity Gas−Liquid Contactor. *Ind. Eng. Chem. Res.* **1990**, *29*, 917.

(6) Singh, S. P.; Wilson, J. H.; Counce, R. M.; Villiers-Fisher, J. F.; Jennings, H. L.; Lucero, A. J.; Reed, G. D.; Ashworth, R. A.; Elliot, M. G. Removal of Volatile Organic Compounds from Groundwater Using a Rotary Air Stripper. *Ind. Eng. Chem.* **1992**, *31*, 574.

(7) Tung, H.-H.; Mah, R. S. H. Modeling Liquid Mass Transfer in Higee Separation Process. *Chem. Eng. Sci.* **1985**, *39*, 147.

(8) Basić, A.; Duduković, M. P. Liquid Holdup in Rotating Packed Beds: Examination of the Film Flow Assumption. *AIChE J.* **1995**, *41*, 301.

(9) Burns, J. R.; Ramshaw, C. Process Intensification: Visual Study of Liquid Maldistribution in Rotating Packed Beds. *Chem. Eng. Sci.* **1996** *51*, 1347.

(10) Liu, H.-S.; Lin, C.-C.; Wu, S.-C.; Hsu, H.-W. Characteristics of a Rotating Packed Bed. *Ind. Eng. Chem. Res.* **1996**, *35*, 3590.

(11) Kelleher, T.; Fair, J. R. Distillation Studies in a High-Gravity Contactor. *Ind. Eng. Chem. Res.* **1996**, *35*, 4646.

(12) Miller, R. W. *Flow Measurement Engineering Handbook*; Mc-Graw Hill Book Company: New York, 1983.

(13) Sharma, M. M.; Gupta, R. K. Mass Transfer Characteristics of Plate Columns without Downcomer. *Trans. Inst. Chem. Eng.* **1967**, *45*, T169.

(14) Sandilya, P. Studies on Gas-phase Mass Transfer in a Centrifugal Contactor. Ph.D. Dissertation, Department of Chemical Engineering, Indian Institute of Technology, Kanpur, India, 1999.

(15) Zheng, C.; Guo, K.; Feng, Y.; Yang, C. Pressure Drop of Centripetal Gas Flow through Rotating Beds. *Ind. Eng. Chem. Res.* **2000**, *39*, 829.

(16) Keyvani, M. Operating Characteristics of Rotating Beds. Ph.D. Dissertation, Department of Chemical Engineering, Case Western Reserve University, Cleveland, OH, 1989.
(17) Lockett, M. J. Flooding of Rotating Structured Packing and its Application to Conventional Packed Columns. *Trans. Inst. Chem. Eng.* **1995**, *73* (A), 379.
(18) Mochizuki, S.; Yang, W.-J. Heat Transfer and Friction Loss in Laminar Radial Flows through Rotating Annular Disks. *Trans. ASME, J. Heat Transfer* **1981**, *103*, 212.
(19) Fogler, H. S. *Elements of Chemical Reaction Engineering*; Prentice Hall of India, 1995.
(20) Strigle, R. F., Jr. *Packed Tower Design and Applications*, 2nd ed.; Gulf Publishing Company: Houston, TX, 1994.
(21) Meier, W.; Stoecker, W. D.; Weinstein, B. Performance of a New, High Efficiency Packing. *Chem. Eng. Sci.* **1977**, *73*, 71.

Received for review January 20, 2000
Revised manuscript received August 29, 2000
Accepted September 12, 2000

IE0000818